Electronic Supplementary Information

Highly luminescent dual-phase $CsPbBr_3/Cs_4PbBr_6$ microcrystals for wide color gamut for backlight display

V. Naresh,*[a] Taehyung Jang,[b] Yoonsoo Pang,[b] and Nohyun Lee*[a]

[a]School of Advanced Materials Engineering, Kookmin University, Seoul 02707, Republic of Korea.

Email: V. Naresh (naresh17@kookmin.ac.kr); Nohyun Lee (nohyunlee@kookmin.ac.kr)

[b]Department of Chemistry, Gwangju Institute of Science and Technology, Gwangju, 61005, Republic of Korea.

Email: Taehyung Jang (taehyungjang@gist.ac.kr); Yoonsoo Pang (ypang@gist.ac.kr)

Materials and chemicals:

Lead bromide ($PbBr_2$, 99.99% Sigma-Aldrich), cesium bromide (CsBr, 99.99% Sigma-Aldrich), N,N-dimethylformamide (DMF, ≥ 99.8% Sigma-Aldrich), and dimethyl sulfoxide (DMSO, ≥ 99.9% Sigma-Aldrich) were purchased and used without further purification.

Synthesis methodology:

Synthesis and purification of dual-phase $CsPbBr_3/Cs_4PbBr_6$: To synthesis dual-phase $CsPbBr_3/Cs_4PbBr_6$, CsBr and $PbBr_2$ were taken in 4:1 molar ratio (i.e. CsBr (16 mmol, 3.405 g), $PbBr_2$ (4 mmol, 1.468 g)) were loaded into a 20 mL vial and 2.5 mL DMF and 2.5 ml DMSO were added. The 20 mL vial containing the precursor salts and solution was subjected to microtip ultrasonication (SONICS, Vibra-Cell, VCX750 ultrasonic processor, 750 W, 20 kHz, see Figure 3a) at a power of 30 W for 30 minutes at room temperature. The precursor salts were added to the solutions and ultrasonicated for 30 min until they were reacted and turned into light greenish-yellow precipitate. The obtained sample was centrifuged at 5000 rpm for 5 min. The supernatant was discarded, and the precipitate was dried in a vacuum oven at 70 °C overnight yielding 0.43 g of $CsPbBr_3/Cs_4PbBr_6$ composite.

Synthesis of $K_2SiF_6:Mn^{4+}$ and $CsPbBr_3/Cs_4PbBr_6$ composite

The $K_2SiF_6:Mn^{4+}$ and $CsPbBr_3/Cs_4PbBr_6$ powders were weighed in different ratios (0.05:1, 0.3:1. 0.6:1, and 0.9:1) and was homogeneously dispersed in the polystyrene-toluene solution (0.1 g of polystyrene granules and 1 mL of toluene). Subsequently, 250 µL of the dispersion was drop-casted on a quartz substrate (13 mm ×13 mm) and naturally dried for 8 hours to remove the solvent. Finally, a uniformly coated $K_2SiF_6:Mn^{4+}$-$CsPbBr_3$/Cs4$PbBr_6$ composite film was obtained.

Fabrication of $K_2SiF_6:Mn^{4+}$-$CsPbBr_3$/Cs4$PbBr_6$ composite coated w-LED device

A prototype white-LED device is fabricated by directly stacking the $K_2SiF_6:Mn^{4+}$-$CsPbBr_3$/Cs4$PbBr_6$ composite coated glasses onto a commercially available blue-emitting InGaN LED chip.

Characterizations:

The samples were synthesized using a 3 mm microtip probe equipped Vibra-Cell (VCX750) ultrasonic processor with an output power of 750 W and frequency of 20 kHz. The XRD patterns of dual-phase $CsPbBr_3/Cs_4PbBr_6$ were recorded on a Bruker DE/D8 Advance X-ray Diffractometer equipped with Cu Kα (λ = 1.541 Å) radiation source operated at 60 kV and 60 mA at room temperature. The samples were provided in dry powder form and scanned within the range of 2θ from 10 to 60°. The morphology of dual-phase $CsPbBr_3/Cs_4PbBr_6$ was investigated from the transmission electron microscopy (TEM) and high-resolution TEM (HR-

TEM) images acquired on a JEM-2100/ JEOL/ JP operated at 200 kV accelerating voltage. The 300 mesh copper Formvar/carbon grid was dipped into the PNCs dispersed toluene solution and allowed to dry in ambient conditions overnight. The X-ray photoelectron spectroscopy (XPS) measurement for dual-phase $CsPbBr_3/Cs_4PbBr_6$ was conducted on an Ulvac PHI/X-tool spectrometer with Al Kα radiation source (1486.6 eV, 24.1W, 15kV) and a beam diameter of 100 μm×100 μm. UV-Vis absorption spectra were measured in the range of 300-700 nm on a Shimadzu UV-2600 spectrometer. The steady-state fluorescence spectra (PL and PLE) were recorded using a Shimadzu RF-6000 Spectro-fluoro-photometer equipped with a 150 W Xe lamp as an excitation and scanning speed of 60,000 nm/min. The time-resolved decay curves of the samples were measured on a HORIBA Jobin Yvon FluoroMax-4 fluorescence spectrometer equipped with a 150 W Xe lamp as an excitation source at room temperature. The PLQY of the dual-phase $CsPbBr_3/Cs_4PbBr_6$ was measured by employing an integrated sphere unit attached to Shimadzu RF-6000 Spectro-fluoro-photometer according to the standard procedure using toluene as a reference under ambient conditions. The stability of the $CsPbBr_3/Cs_4PbBr_6$ composite in different conditions (ultraviolet (UV) light irradiation, moisture tolerance, and thermal resistance) are comparably analyzed with monoclinic $CsPbBr_3$. The photostability test was carried out for $CsPbBr_3$ and $CsPbBr_3/Cs_4PbBr_6$, by continuous irradiating with a UV lamp (365 nm, 6W), placed at a distance of 1 cm for 120 hours. The effect of moisture on the $CsPbBr_3$ and $CsPbBr_3/Cs_4PbBr_6$ was evaluated by storing them in an unsealed vial under ambient conditions (at 25 °C, relative humidity of 70%) for a period of time (150 min). The temperature stability test was carried out for $CsPbBr_3$ and $CsPbBr_3/Cs_4PbBr_6$ by heating at 120 °C for 24 hours under ambient conditions.

Table S1: The average lifetimes (τ_{avg}) of PL decay curves and photoluminescence quantum yield (PLQYs) for $CsPbBr_3$ and $CsPbBr_3$/ Cs_4PbBr_6.

Sample	**A_1**	**τ_2 (ns)**	**A_2**	**τ_2 (ns)**	**τ_{avg} (ns)**	**PLQY (%)**
$CsPbBr_3$	0.5794	2.9694	0.3915	16.6056	13.7521	46.2
$CsPbBr_3$/ Cs_4PbBr_6	0.4929	6.47	0.58157	31.3172	27.6149	82.7

Table S2: The luminous efficacy (LE), chromaticity coordinates, correlated color temperature (CCT), color rendering index (CRI), color gamut (NTSC %) of the LED devices constructed using the different weight ratio of $K_2SiF_6:Mn^{4+}$ to $CsPbBr_3/Cs_4PbBr_6$ under 20 mA forward-bias current (after color filtering in the constructed LEDs).

Weight ratio of $K_2SiF_6:Mn^{4+}$ to $CsPbBr_3/Cs_4PbBr_6$	LE ($lm\ W^{-1}$)	Chromaticity coordinates (x, y)	CCT (K)	CRI	Color gamut (NTSC %)
0.05:1	101	0.2252, 0.3297	12,771	74	121.04
0.3:1	68	0.3218, 0.3402	5,564	87	118.78
0.6:1	56	0.3975, 0.3701	3,514	93	116.79
0.9:1	42	0.5319, 0.3847	1,815	95	113.23

Table S3. The comparison of the color coordinates, luminescence efficiency (LE), correlated color temperature (CCT), and the color gamut of w-LEDs constructed using various luminescent materials combinations (quantum dots converted W-LEDs).

W-LED system	Color coordinates (x,y)	LE(lm/W)	CCT(K)	Color gamut (% NTSC)	Reference
YAG:Ce^{3+}	(0.296, 0.295)	105.0	8245	67.9	[1, 2]
$CsPbBr_3$+K_2SiF_6:Mn^{4+}	(0.271, 0.232)	37.0	-	89%	[3]
$CsPbBr_3$+$CsPb(Br/I)_3$	(0.24, 0.28)	30.0	-	113.0	[4]
$CsPbBr_3$/PSZ QDs+K_2SiF_6:Mn^{4+}	(0.308, 0.328)	138.6	6762	111.0	[5]
$CsPbBr_3$-DG+K_2SiF_6:Mn^{4+} PiG	(0.238, 0.347)	90.9	10,952	103.1	[6]
$CsPbBr_3$+$CsPb(Br_{1.2}/I_{1.8})$	(0.33, 0.34)	51	5516	122	[7]
$CsPbBr_3$/$CsPb_2Br_5$				134.2	[8]
$CsPbBr_3$/Cs4$PbBr_6$+ K_2SiF_6:Mn^{4+}	(0.39, 0.37)	88		131	[9]
$CsPbBr_3$–PMMA+ K_2SiF_6:Mn^{4+}	(0.324, 0.321)		5955.42		[10]
$MAPbBr_3$/PVDF+ K_2SiF_6:Mn^{4+}	0.272, 0.278)	109		121	[11]
Cs4$PbBr_6$/$CsPbBr_3$+ K_2SiF_6:Mn^{4+}		73.8			[12]
$CsPbBr_3$/TDPA QDs+ K_2SiF_6:Mn^{4+}	(0.31, 0.29)	63	7072	122	[13]
$CsPbBr_3$/Cs_4PbBr_6+ K_2SiF_6:Mn^{4+}	(0.331, 0.328)	68	5,564	188.78	This work

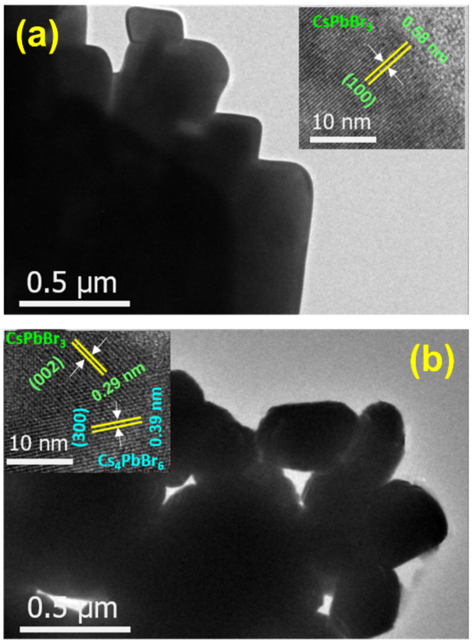

Figure S1. TEM images of the samples obtained after reaction times of (a) 3 min, (b) 10 min (inset corresponding HR-TEM images).

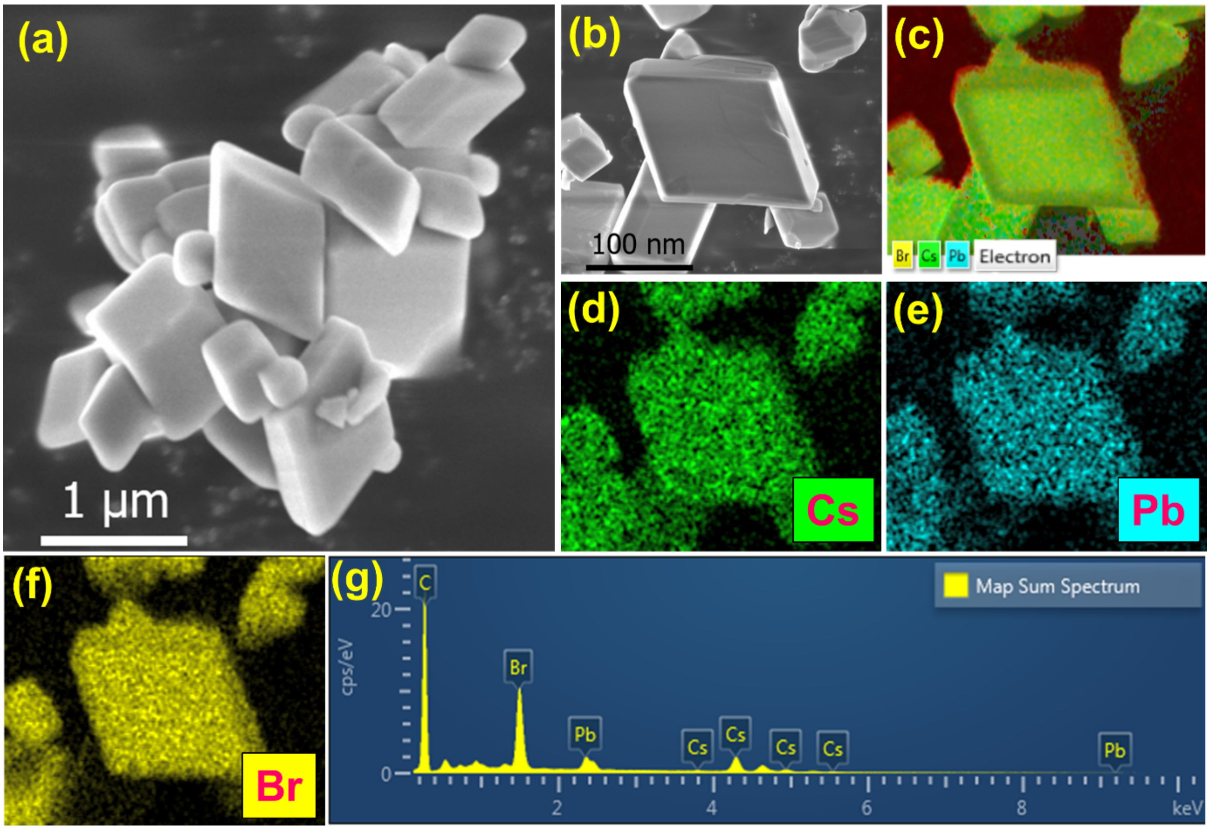

Figure S2. (a) Low- and (b) high- magnification field-emission scanning electron microscopy images of $CsPbBr_3$ embedded Cs_4PbBr_6 MCs, (c-f) mapping of elements Cs (green), Pb (cyan), and Br (yellow), (g) energy-dispersive spectrum of Cs_4PbBr_6 MCs embedded with $CsPbBr_3$.

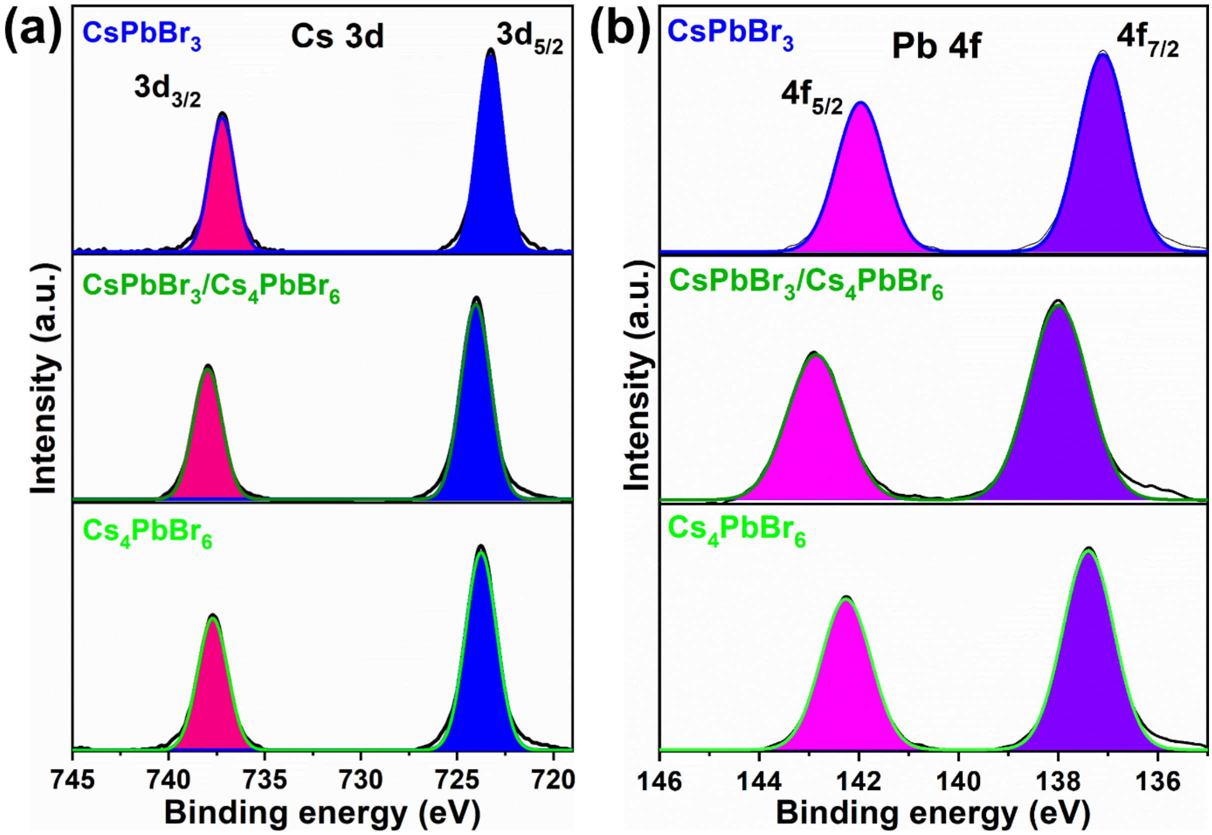

Figure S3. High-resolution X-ray photoelectron spectra corresponding to elements (a) Cs (3d), and (b) Pb (4f).

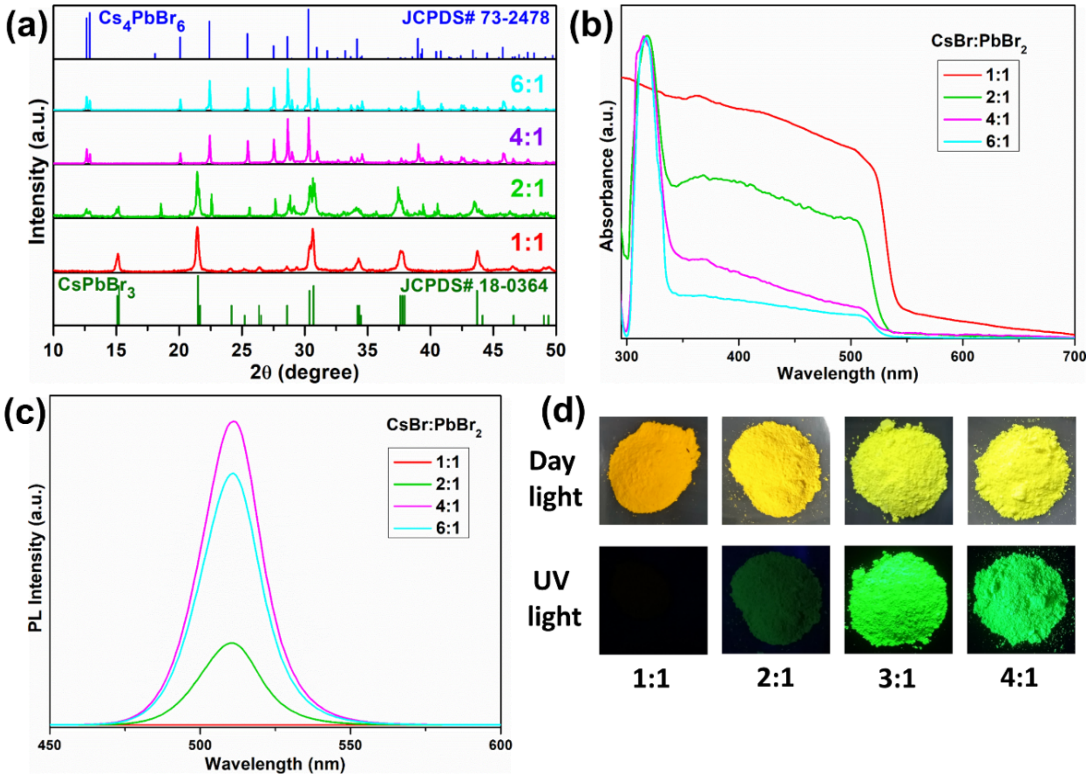

Figure S4. (a) XRD pattern, (b) absorption spectra, (c) PL spectra (d) photographs under day and UV light of the products, when CsBr and $PbBr_2$ taken different molar ratios (1:1, 2:1, 4:1, and 6:1). The XRD pattern are well indexed to JCPDS# 18-0364 ($CsPbBr_3$), and JCPDS# 73-2478 (Cs_4PbBr_6).

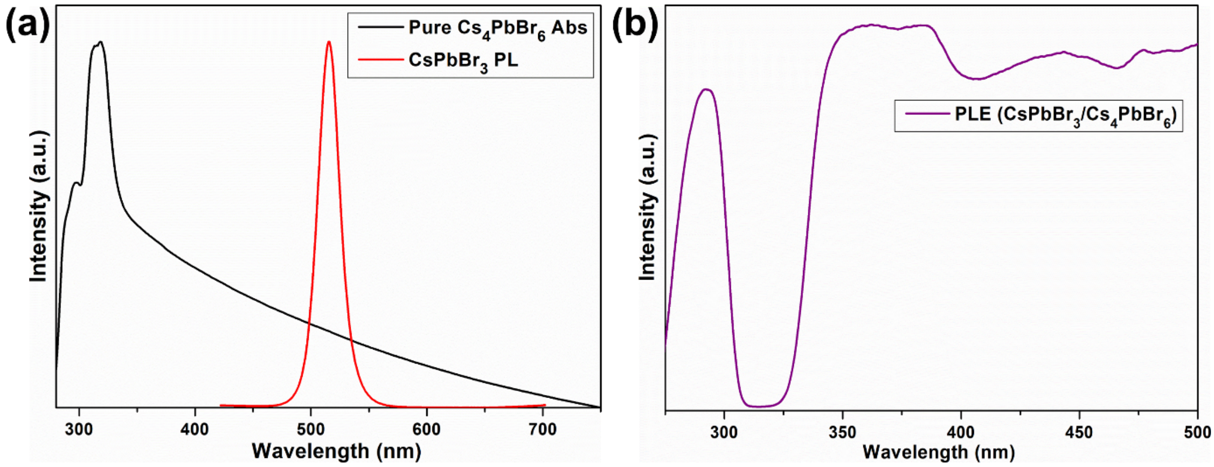

Figure S5. (a) Overlap of absorption spectrum of pure Cs_4PbBr_6 and PL spectrum of $CsPbBr_3$, (b) PLE spectrum of the $CsPbBr_3/Cs_4PbBr_6$ MCs when monitored with green emission wavelength (505 nm) of $CsPbBr_3$.

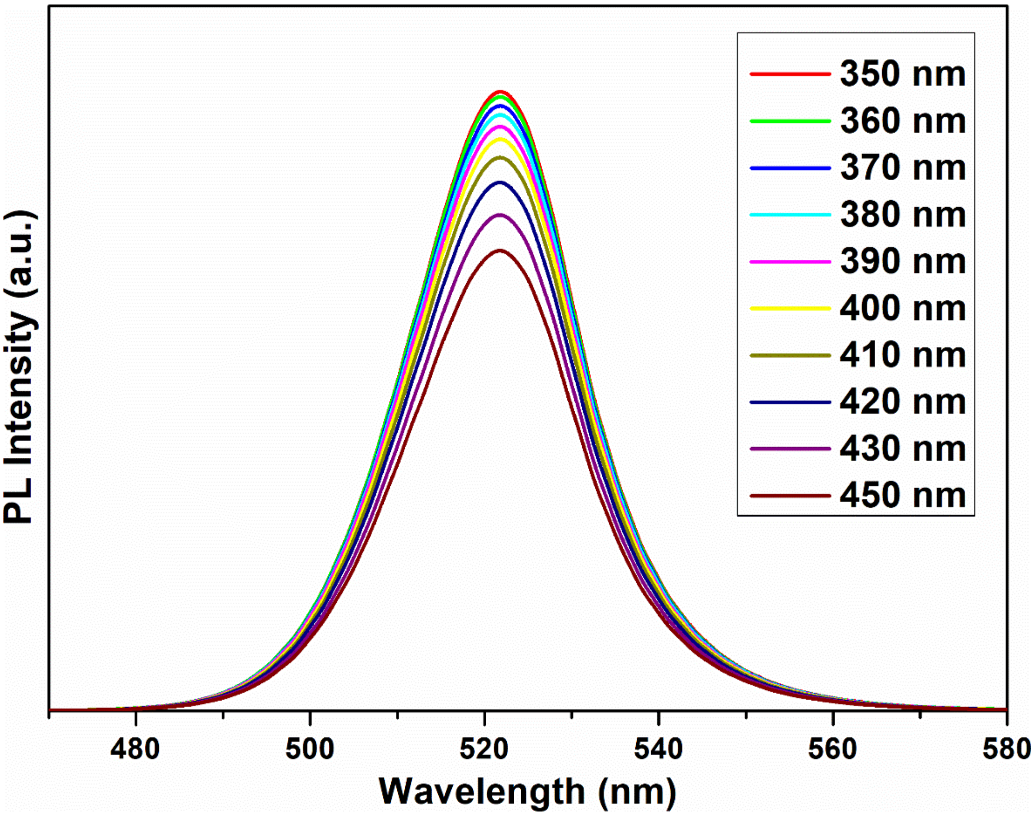

Figure S6. Photoluminescence spectra of dual-phase $CsPbBr_3/Cs_4PbBr_6$ MCs under different excitation wavelengths (350-450 nm).

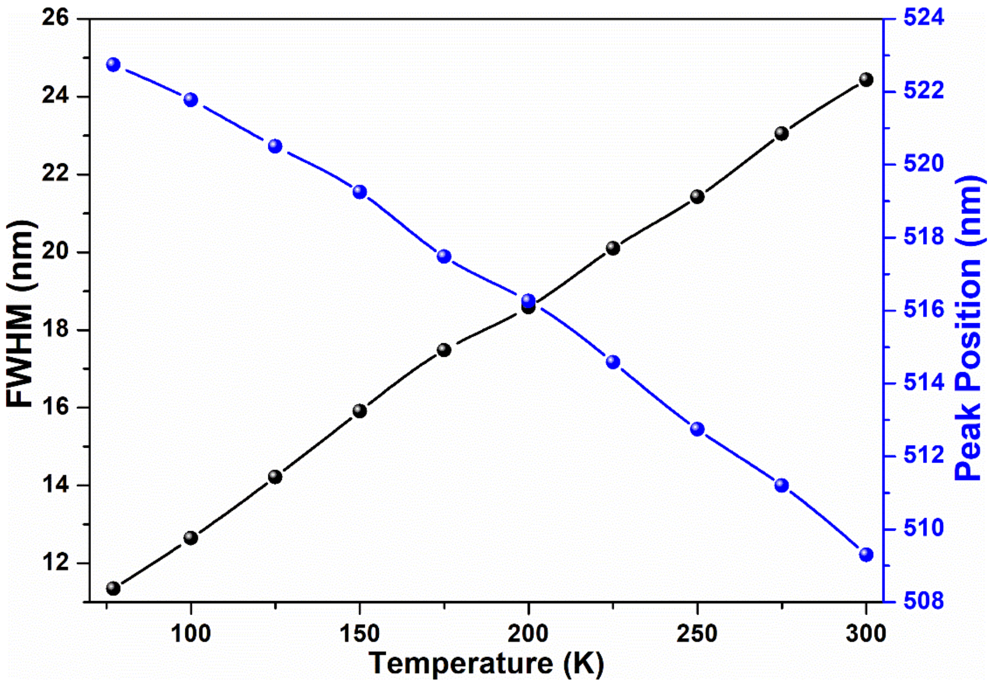

Figure S7. Temperature-dependent FWHM and peak position of the green color emitting peak of $CsPbBr_3/Cs_4PbBr_6$ MCs.

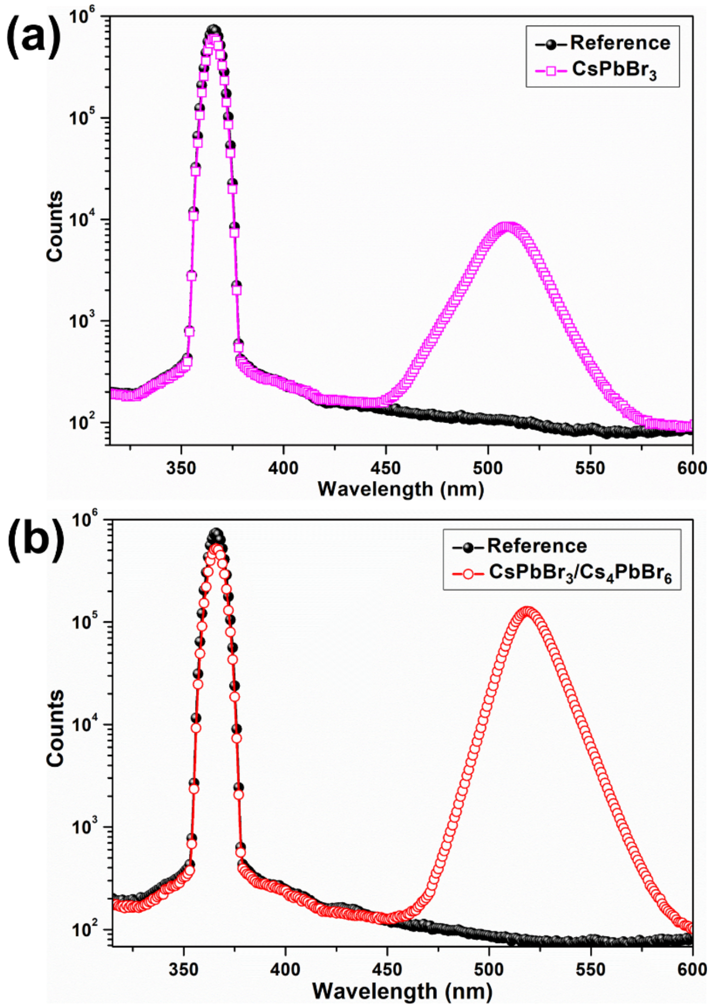

Figure S8. Photoluminescence quantum yield (PLQY) of (a) $CsPbBr_3$ NCs and (b) dual-phase $CsPbBr_3/Cs_4PbBr_6$ MCs.

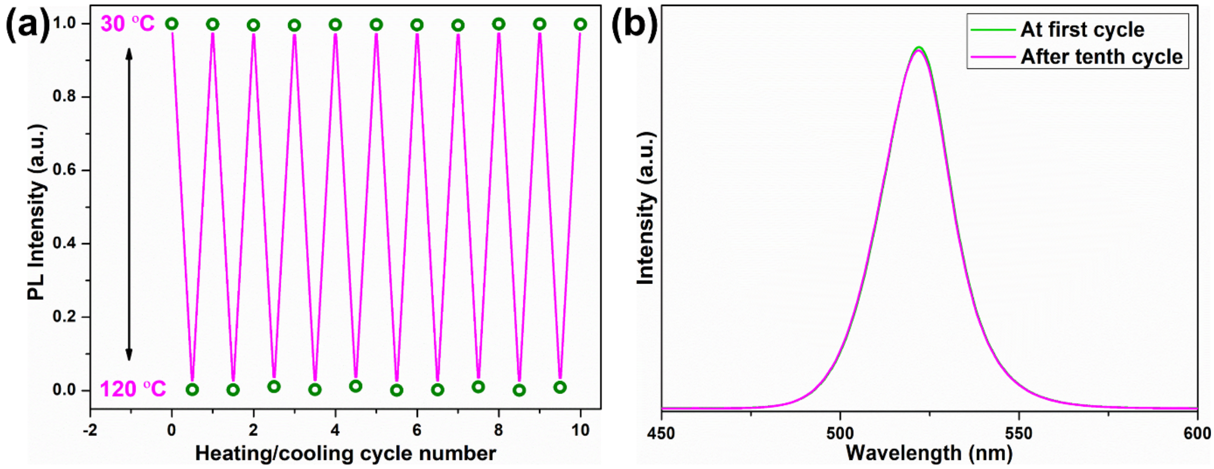

Figure S9. Thermal recovery (luminescence quenching and recovery) test for the dual-phase $CsPbBr_3/Cs_4PbBr_6$ MCs between 30-120 °C for 10 cycles of heating and cooling, (b) Photoluminescence spectra of dual-phase $CsPbBr_3/Cs_4PbBr_6$ MCs at the start of the first cycle and after the tenth cycle.

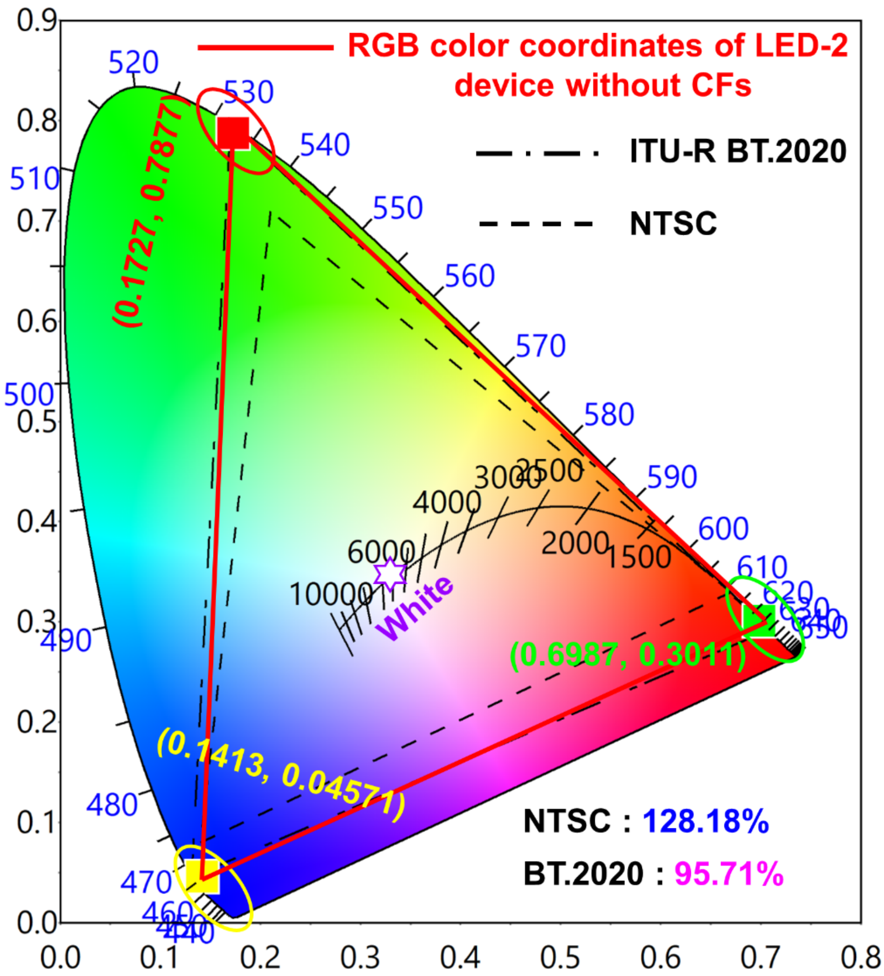

Figure S10. CIE color coordinates of unfiltered RGB EL spectra of white light-emitting LED 2 device and comparison of the wide color gamut of blue-chip + green-emitting $CsPbBr_3/Cs_4PbBr_6$ + red-emitting $K_2SiF_6:Mn^{4+}$ with NTSC standard triangle (----), and ITU-R BT.2020 (Rec. 2020) triangle (− · − · −).

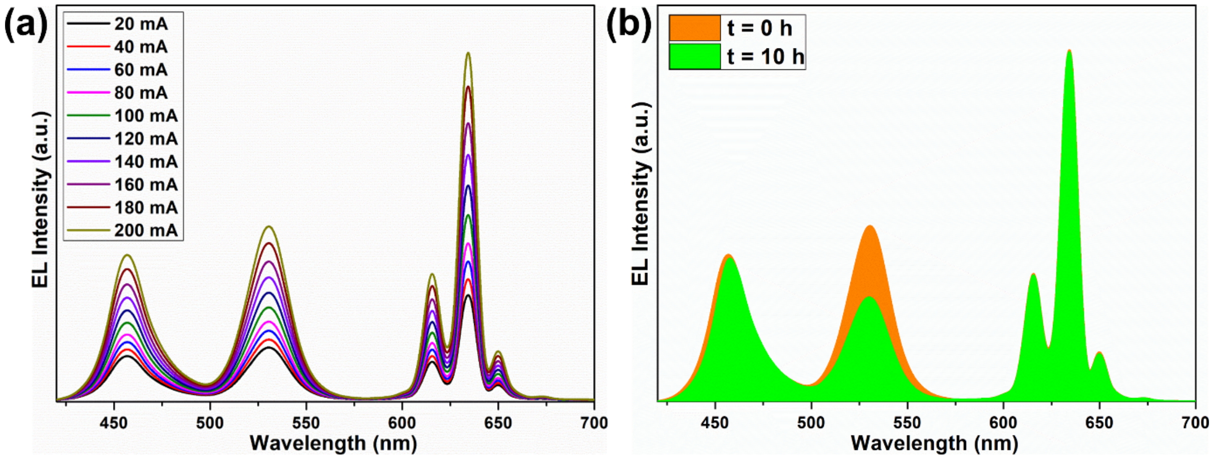

Figure S11. (a) EL spectra of white LED 2 device constructed with the composite ratio of 0.3:1 (K_2SiF_6:Mn^{4+}: $CsPbBr_3$/Cs_4PbBr_6) under various operating currents and (b) EL spectra measured at two different time intervals (t = 0 and 10 h) under 70% RH.

References

1 K. Li, C. Shen, *Optik,* 2012, **123**, 621–623.

2 J. H. Oh, H. Kang, M. Ko, Y. R. Do, *Opt. Express,* 2015, **23**, 791.

3 X. J. Zhang, H. C. Wang, A. C. Tang, S. Y. Lin, H. C. Tong, C. Y. Chen, Y. C. Lee, T. L. Tsai, R. S. Liu, *Chem. Mater.,* 2016, **28**, 8493–8497.

4 H. C. Wang, S. Y. Lin, A. C. Tang, B. P. Singh, H. C. Tong, C. Y. Chen, Y. C. Lee, T. L. Tsai, R. S. Liu, *Angew. Chem. Int. Ed.,* 2016, **55**, 1–6.

5 Z. Luo, Y. Chen, S. T. Wu, *Opt. Express,* 2013, **21**, 26269–26284.

6 H. C. Yoon, S. Lee, J. K. Song, H. Yang, Y. R. Do, *ACS Appl. Mater. Interfaces,* 2018, **10**, 11756–11767.

7 C. H. Lin, A. Verma, C. Y. Kang, Y. M. Pai, T. Y. Chen, J. J. Yang, C. W. Sher, Y. Z. Yang, P. T. Lee, C. C. Lin, Y, C. Wu, S. K. Sharma, T. Wu, S. R. Chung, H. C. Kuo, *Photon. Res*., 2019**,** **7**, 579–585.

8 H. C. Yoon, H. Lee, H. Kang, J. H. Oha, Y. R. Do, *J. Mater. Chem. C*, 2018, **6**, 13023–13033.

9 W. Wang, D. Wang, F. Fang, S. Wang, G. Xu, T. Zhang, *Cryst. Growth Des.* 2018, **18**, 6133–6141.

10 Y. Xin, H. Zhao, J. Zhang, *ACS Appl. Mater. Interfaces,* 2018, **10**, 4971–4980.

11 Q. Zhou, Z. Bai, W. G. Lu, Y. Wang, B. Zou, H. Zhong, *Adv. Mater.,* 2016, **28**, 9163–9168.

12 Y. M. Chen, Y. Zhou, Q. Zhao, J. Y. Zhang, J. P. Ma, T. T. Xuan, S. Q. Guo, Z. J. Yong, J.Wang, Y. Kuroiwa, C. Moriyoshi, H. T. Sun, *ACS Appl. Mater. Interfaces,* 2018, **10**, 15905–15912.

13 T. Xuan, X. Yang, S. Lou, J. Huang, Y. Liu, J. Yu, H. Li, K. L. Wong, C. Wang, J. Wang, *Nanoscale* 2017**,** **9**, 15286–15290.